

# Discordant asymmetries of synaptic density, blood flow and glucose metabolism in temporal lobe epilepsy: a combined [<sup>11</sup>C]UCB-J and [<sup>18</sup>F]FDG PET study

Volpi Tommaso<sup>1</sup>, Imran Quraishi<sup>2</sup>, Sjoerd J. Finnema<sup>3</sup>, Kamil Detyniecki<sup>4</sup>, Dennis D. Spencer<sup>5</sup>, Richard E. Carson<sup>1</sup>, Takuya Toyonaga<sup>1</sup>

1. PET Center, Department of Radiology and Biomedical Imaging, Yale University, New Haven, CT
2. Department of Neurology, Yale University, New Haven, CT
3. Integrated Science and Technology, Translational Imaging, AbbVie, North Chicago, IL
4. Department of neurology, University of Miami Miller School of Medicine, Miami, FL
5. Department of Neurosurgery, Yale University, New Haven, CT

## Purpose/Background

Temporal lobe epilepsy (TLE) originates from a seizure onset zone (SOZ) which is typically located in the medial temporal lobe (MTL). In previous work, we have shown how [<sup>11</sup>C]UCB-J SV2A-PET synaptic density estimates display higher hippocampal asymmetry than [<sup>18</sup>F]FDG glucose metabolism in TLE, which might be helpful for preoperative localization of the SOZ [1]. Here, we explored asymmetries in other regions of interest (ROIs), both in the cortex and subcortex, which might provide interesting insights, e.g., in the thalamus, which was found to be significantly affected in TLE [2].

## Methods

Eleven patients with TLE (39 ± 11 years old, 5 F) were recruited (inclusion criteria: SOZ in the MTL, and MRI findings of mesial temporal sclerosis). T1w MRI images were acquired on a Siemens TrioTrim scanner. [<sup>11</sup>C]UCB-J PET data were acquired on a HRRT scanner for 60 min. Partial volume correction (PVC) of [<sup>11</sup>C]UCB-J dynamic images was performed with the Iterative Yang algorithm [3]. A 1-tissue compartment model with metabolite-corrected input function was fitted at the voxel level to estimate distribution volume ( $V_T$  [ml/cm<sup>3</sup>]) and inflow rates ( $K_1$  [ml/cm<sup>3</sup>/min]); the binding potential ( $BP_{ND}$  [unitless]) was calculated using the centrum semiovale as a reference region [4]. [<sup>18</sup>F]FDG PET acquisitions were performed either on the HRRT (n = 8) or a Discovery PET/CT scanner (n = 3), and, after PVC, standardized uptake values (SUV [kg/mL]) were obtained from 30-60 min and 50-60 min post-injection windows, respectively. After T1w segmentation with Freesurfer 6.0, and linear PET-to-T1w mapping, average  $BP_{ND}$ ,  $K_1$  and SUV values were extracted for 12 temporal and subcortical ROIs. Regional asymmetry indices (AIs) were calculated as  $100\% \times [\text{contralateral} - \text{ipsilateral}]/\text{contralateral}$  for each parameter, and the sign of the median AI values across subjects was evaluated. For each region, pairwise correlations between AI values of different parameters were assessed across patients.

## Results

Boxplots of the AIs are reported in **Figure 1**. Median AIs are positive in virtually all regions for both [<sup>11</sup>C]UCB-J  $K_1$  and [<sup>18</sup>F]FDG SUV, and in thalamus and anteromedial temporal lobe for [<sup>11</sup>C]UCB-J  $BP_{ND}$ , which however has negative AIs in the remaining areas. When we evaluated the ROI-wise association between AI values from different parameters, strong

linear relationships ( $R^2 > 0.7$ ) were observed in the thalamus between  $BP_{ND}$ ,  $K_1$  and SUV AIs (both with and without PVC), higher than in the hippocampus (**Figure 2**). No significant inter-parameter associations were detected in the remaining regions. Moreover, thalamus AIs did not correlate with hippocampus AIs for any of the parameters.

## Conclusion

As expected, TLE patients have positive AIs for [ $^{11}\text{C}$ ]UCB-J  $K_1$  and [ $^{18}\text{F}$ ]FDG SUV (proxies of blood flow and glucose metabolism, respectively). Many negative AIs are found for  $BP_{ND}$  in insula and posterolateral temporal cortex, indicating higher synaptic density in the hemisphere ipsilateral to the SOZ and thus, possibly, compensatory synaptic remodeling. We also found highly consistent asymmetry in measures of *synaptic structure* ( $BP_{ND}$ ) and *function* ( $K_1$  and SUV) in the thalamus, even higher than in hippocampus. This adds to previous work reporting that thalamic asymmetries on [ $^{18}\text{F}$ ]FDG PET were predictive of seizure recurrence in TLE [5]. Of note, the range of thalamic AI values is smaller than in hippocampus: this could depend on the thalamic ROI, with previous findings showing selective involvement of thalamic nuclei in TLE [2]. These results enrich our understanding of how *synaptic structural* and *functional* measures relate to one another in disease. Future work should explore if asymmetries in the thalamus can predict clinical scores (e.g., seizure severity), and whether this pattern relates to asymmetries in other regions.

1. <https://doi.org/10.1111/epi.16653>
2. <https://doi.org/10.1111/epi.12520>
3. <https://doi.org/10.1016/j.neuroimage.2021.118248>
4. <https://doi.org/10.1177/0271678x19879230>
5. PMID:11138679

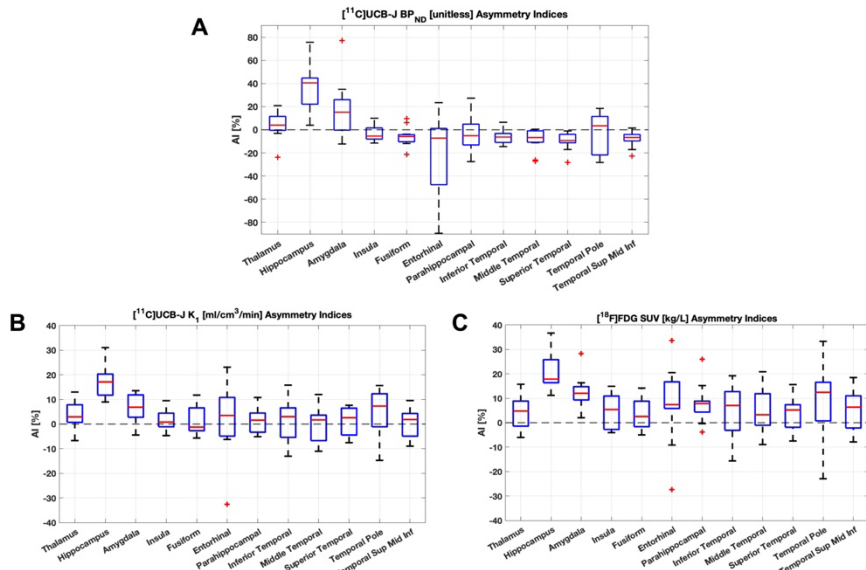


**Figure 1.** Boxplots of the AIs ([unitless]) for 12 ROIs:  $[^{11}\text{C}]\text{UCB-J } BP_{\text{ND}}$  (A),  $[^{11}\text{C}]\text{UCB-J } K_1$  (B) and  $[^{18}\text{F}]\text{FDG SUV}$  (C). The median AI values across subjects are shown as red central marks for each boxplot/region.

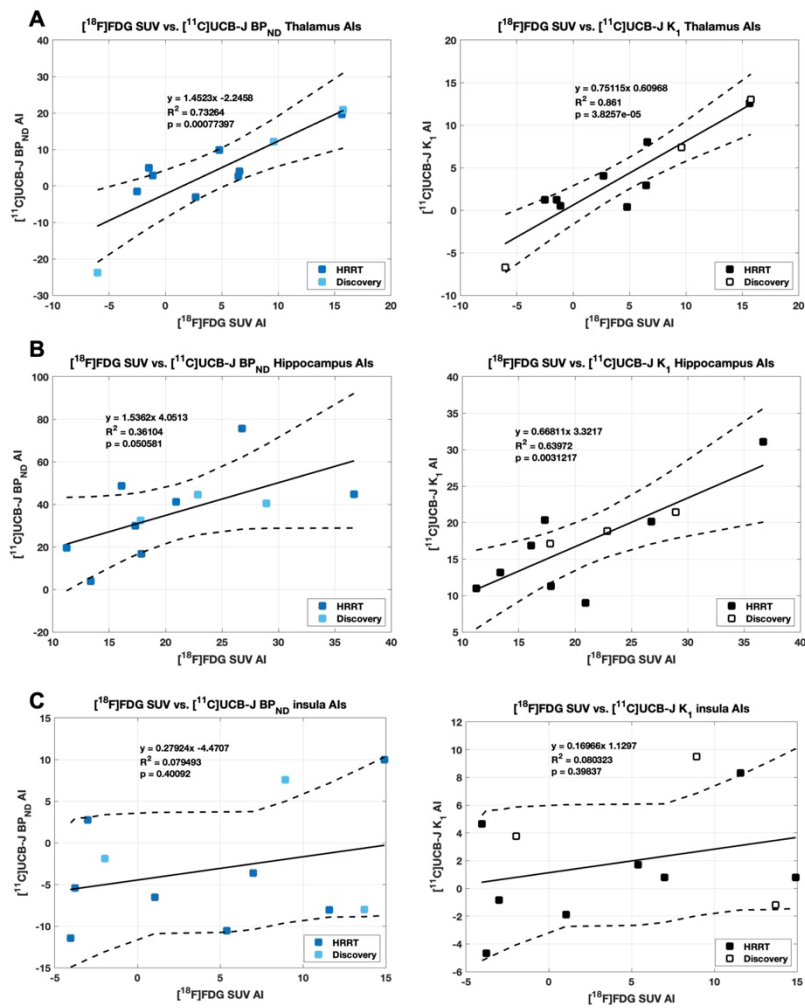


**Figure 2.** Scatter plots of the relationship between the AI values of SUV vs.  $BP_{\text{ND}}$  (left panels), and SUV vs.  $K_1$  (right panels) in thalamus (A), hippocampus (B), insula (C) across TLE patients (partitioned according to the scanner where  $[^{18}\text{F}]\text{FDG}$  PET was acquired, i.e., HRRT or Discovery). The regression line (continuous) is shown with its 95% confidence intervals (dashed lines). The insula is shown because it has similar AI range as the thalamus, but without any inter-parameter association.